SLAC–PUB–5151
December 1989
(T/E)

UPDATE ON K^* STUDIES AT SLAC*

D. ASTON,[1] N. AWAJI,[2] T. BIENZ,[1] F. BIRD,[1] J. D'AMORE,[3]
W. DUNWOODIE,[1] R. ENDORF,[3] K. FUJII,[2] H. HAYASHII,[2] S. IWATA,[2]
W.B. JOHNSON,[1] R. KAJIKAWA,[2] P. KUNZ,[1] Y. KWON,[1] D.W.G.S. LEITH,[1,◇]
L. LEVINSON,[1] T. MATSUI,[2] B.T. MEADOWS,[3] A. MIYAMOTO,[2] M. NUSSBAUM,[3]
H. OZAKI,[2] C.O. PAK,[2] B.N. RATCLIFF,[1] P. RENSING,[1] D. SCHULTZ,[1]
S. SHAPIRO,[1] T. SHIMOMURA,[2] P. K. SINERVO,[1] A. SUGIYAMA,[2] S. SUZUKI,[2]
G. TARNOPOLSKY,[1] T. TAUCHI,[2] N. TOGE,[1] K. UKAI,[4] A. WAITE,[1] and S. WILLIAMS[1]

[1] *Stanford Linear Accelerator Center, Stanford University, Stanford, CA 94309*
[2] *Nagoya University, Furo-cho, Chikusa-ku, Nagoya 464, Japan*
[3] *University of Cincinnati, Cincinnati, OH 45221*
[4] *Institute for Nuclear Study, University of Tokyo, Midori-cho, Tanashi, Tokyo 188, Japan*

ABSTRACT

Results from the systematic study of K^* spectroscopy, by the LASS group, are reviewed. New data from the study of the reaction $K^-p \to \bar{K}^0\pi^-p$ are presented, and compared to our previous results. Confirmation of three new K^* excited states is presented.

INTRODUCTION

The LASS experiment at the Stanford Linear Accelerator Center has been performing a systematic study of K^* spectroscopy over the past few years, using data from a high statistics K^-p run at 11 GeV/c. Progress on our studies of the strangeonium sector was reported in a talk by Blair Ratcliff,[1)] at this conference. The results on K^* states studied so far are summarized in Fig. 1, where the full spectrum of the expected K^* states is displayed, and those found in our LASS experiment are marked as boxes.[2-5)] These results come mainly from the study of the following reactions:

$$K^-p \to K^-\pi^+n \quad (1)$$

$$\to \bar{K}^0\pi^+\pi^-n \quad (2)$$

$$\to K^-\pi^+\pi^-\pi^0p \quad . \quad (3)$$

⋆ Work supported by Department of Energy contract DE–AC03–76SF00515; the National Science Foundation under Grants PHY82–09144 and PHY85–13808; and the Japan–U.S. Cooperative Research Project on High Energy Physics.

◇ Presented by D.W.G.S. Leith.

Invited talk presented at the HADRON89: 3rd International Conference on Hadron Spectroscopy, Ajaccio, France, September 23–27, 1989

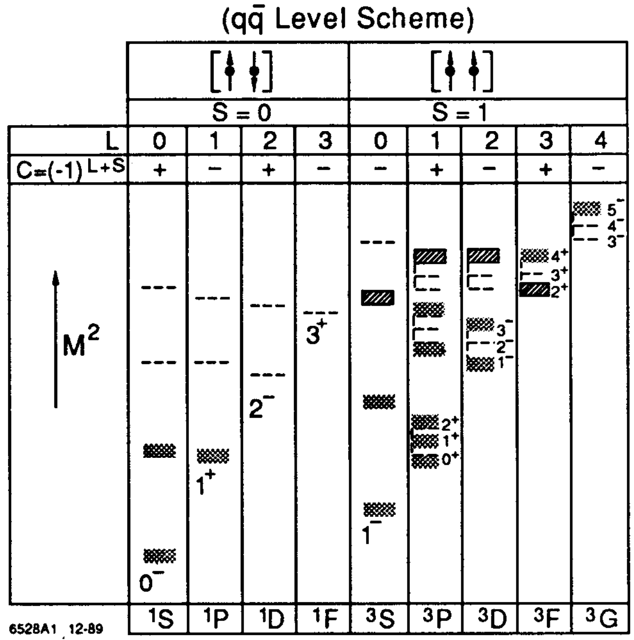

Figure 1. The expected spectrum of K^* states for both natural and unnatural spin-parities. The boxes represent the states found, and studied, in the LASS experiment at SLAC.

The $K\pi$ elastic partial wave amplitudes,[2,5] derived from the data of reaction (1), are displayed in Fig. 2. The leading partial waves from reactions (2) and (3) are shown in Figs. 3 and 4, for the inelastic final states $K^*\pi$, $K\rho$[3,5] and $K\eta$,[4,5] respectively. From the energy dependence of these amplitudes the leading states $K^*(892)$, $K_2^*(1430)$, $K_3^*(1780)$, $K_4^*(2075)$ and $K_5^*(2380)$ have been identified. In addition, the radial excitation of $K^*(892)$ at 1400 MeV/c^2, the probable radial excitation of the $K_2^*(1430)$ at 1970 MeV/c^2, the scalar $J^P = 0^+$ at 1400 MeV/c^2 and its radial excitation at 1950 MeV/c^2, and the vector ($J^P = 1^-$) state at 1700 MeV/c^2, presumably the (L-S) state associated with the $K_3^*(1780)$ have also been identified. These states are marked in Fig. 1 as solid boxes, and are in rather good standing. Indications for a second radial excitation of the $K^*(892)$ at a mass around 2050 MeV/c^2 and a possible radial excitation of the $K_3^*(1780)$ at a mass around 2100 MeV/c^2 are also seen in our data. They are indicated as shaded regions in Fig. 1, and certainly require confirmation by observation in other channels and in other experiments.

NEW DATA ON $K^-p \to \bar{K}^0\pi^-p$

We present new data on a study of the reaction[6]

$$K^-p \to \bar{K}^0\pi^-p \quad , \tag{4}$$

a reaction *not* dominated by one pion exchange, but by isoscalar, natural J^P exchange.

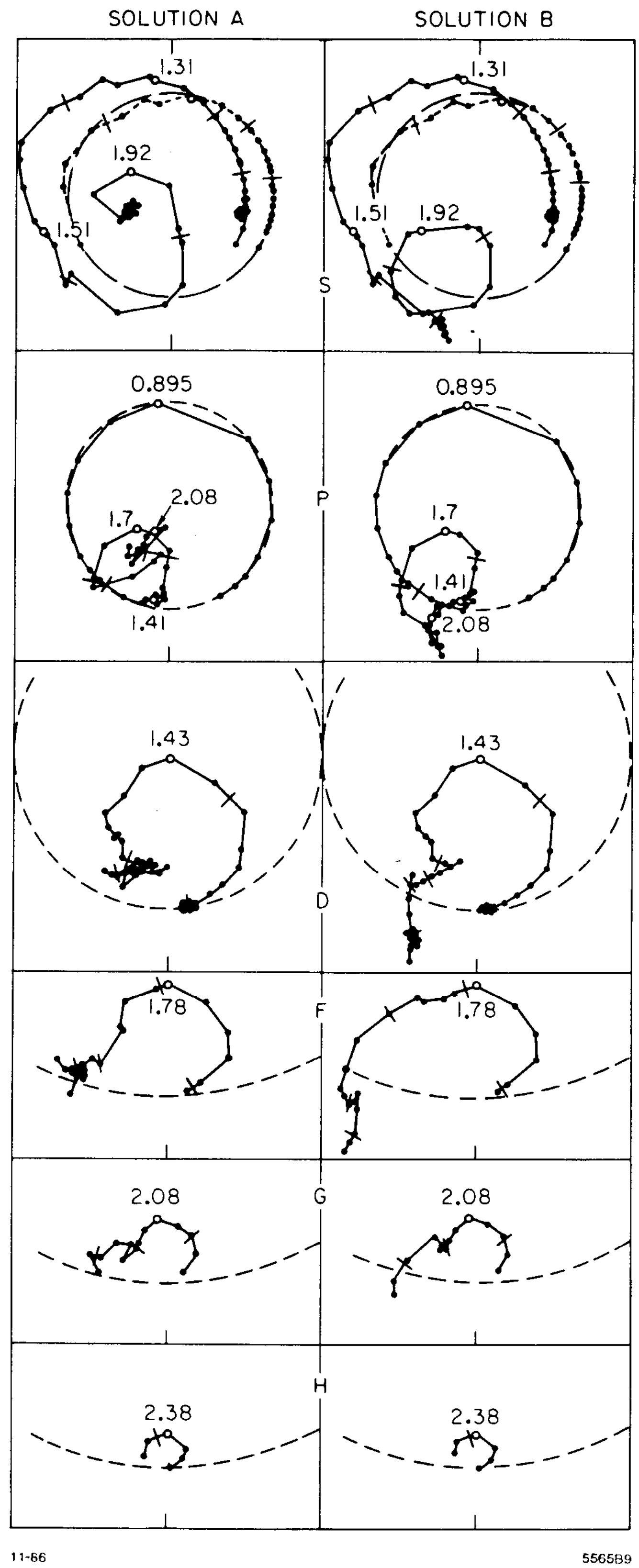

Figure 2. The $K\pi$ elastic scattering amplitude from threshold up to 2500 MeV/c^2, showing the resonant structure in all partial waves up to $J^P = 5^-$. The results are from the LASS analysis of the reaction $K^- p \to K^- \pi^+ n$ at 11 GeV/c.[2]

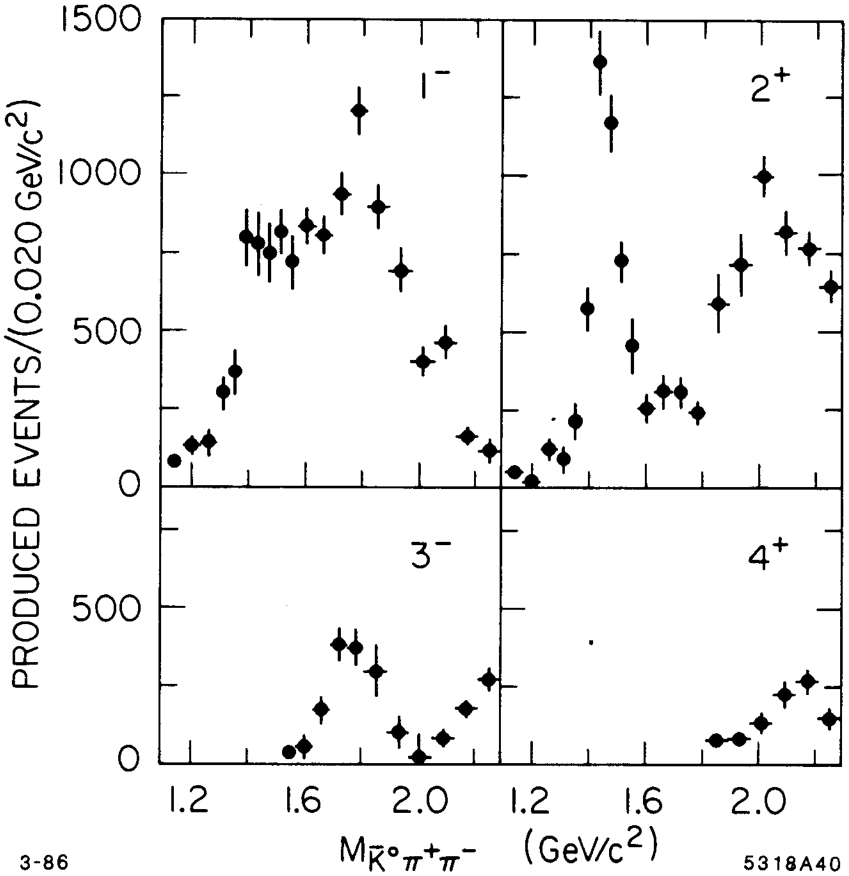

Figure 3. The partial wave amplitudes for the natural parity K^* waves, from an analysis of the reaction $K^- p \to \bar{K}^0 \pi^+ \pi^- n$ at 11 GeV/c, by the LASS experiment at SLAC.[3]

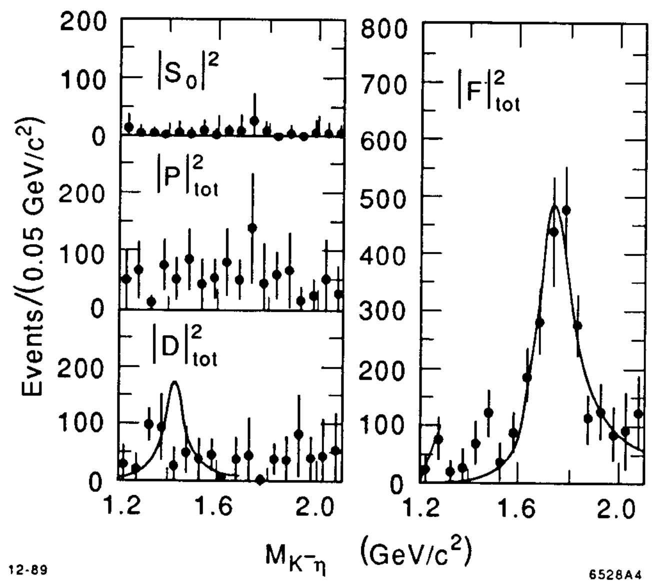

Figure 4. The partial wave amplitudes for the $K^{*-} \to K^- \eta$ system, as derived from analysis of the reaction $K^- p \to K^- \pi^+ \pi^- \pi^0 p$ at 11 GeV/c, by the LASS experiment at SLAC.[4]

The Dalitz plot for this reaction is shown in Fig. 5, where the N^* and K^* bands are clearly visible. The decay distribution data for the K^*'s, are shown in Figs. 6 and 7, as a

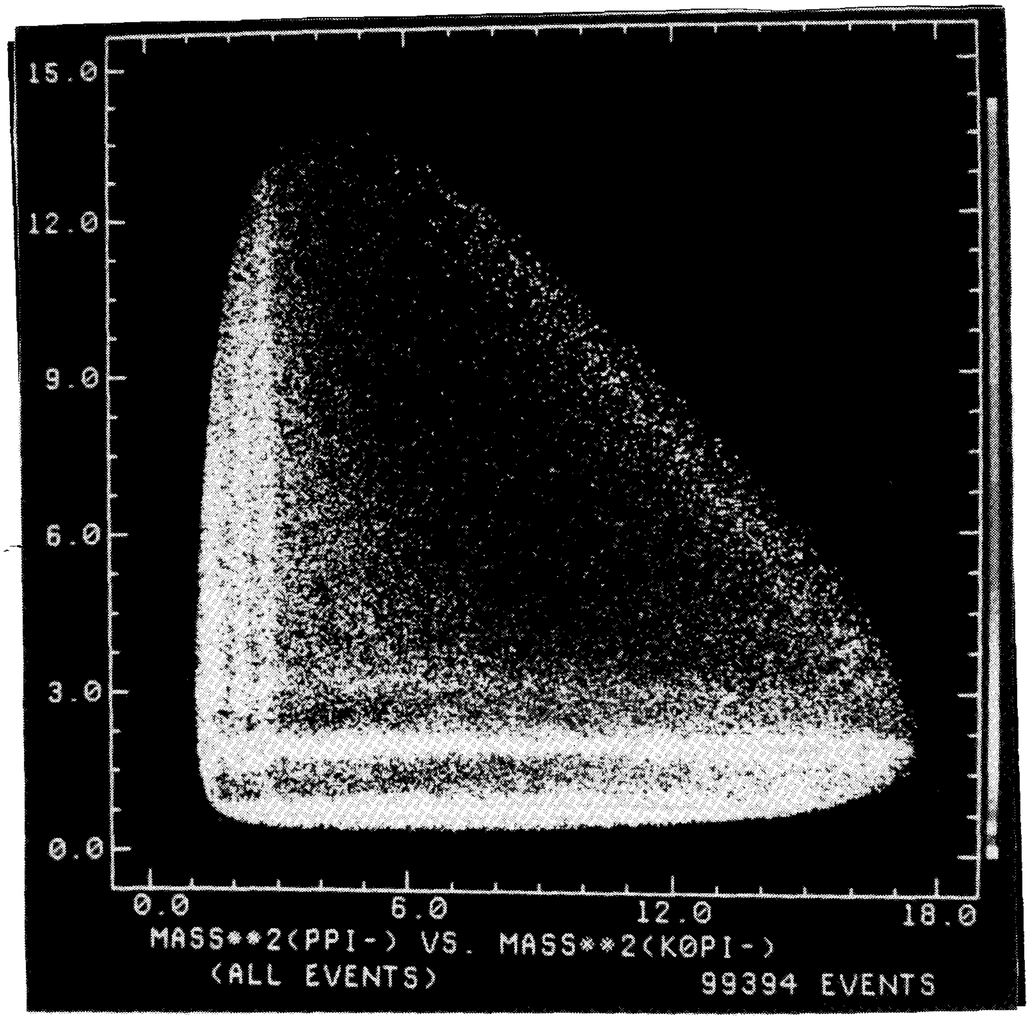

Figure 5. *The Dalitz plot from the reaction* $K^- p \to \bar{K}^0 \pi^- p$.

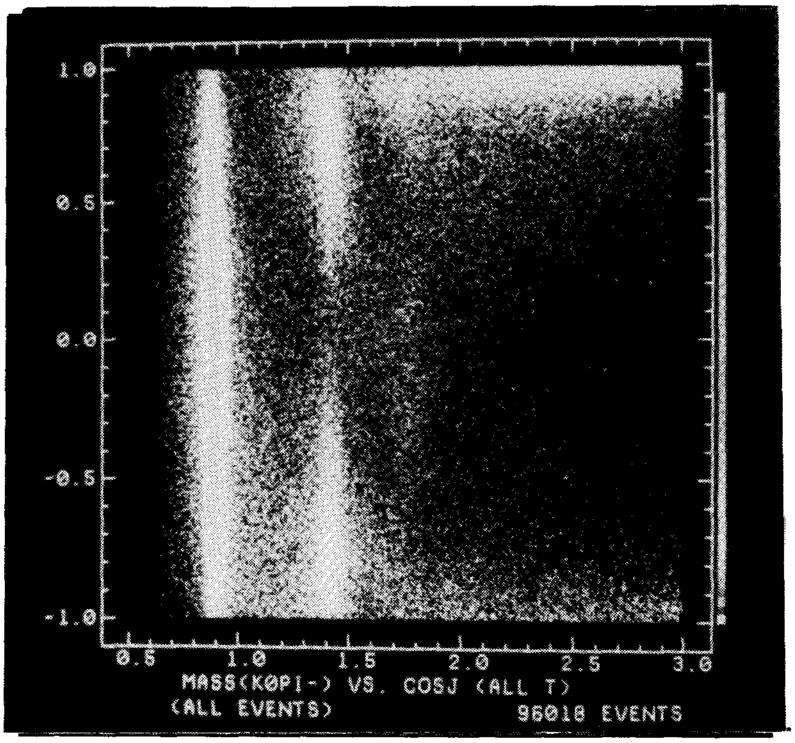

Figure 6. *The decay distribution of* $K^{*-} \to \bar{K}^0 \pi^-$ *is shown in a scatterplot of the cosine of the Jackson angle in the* $K\pi$ *center-of-mass, as a function of* $K\pi$ *mass.*

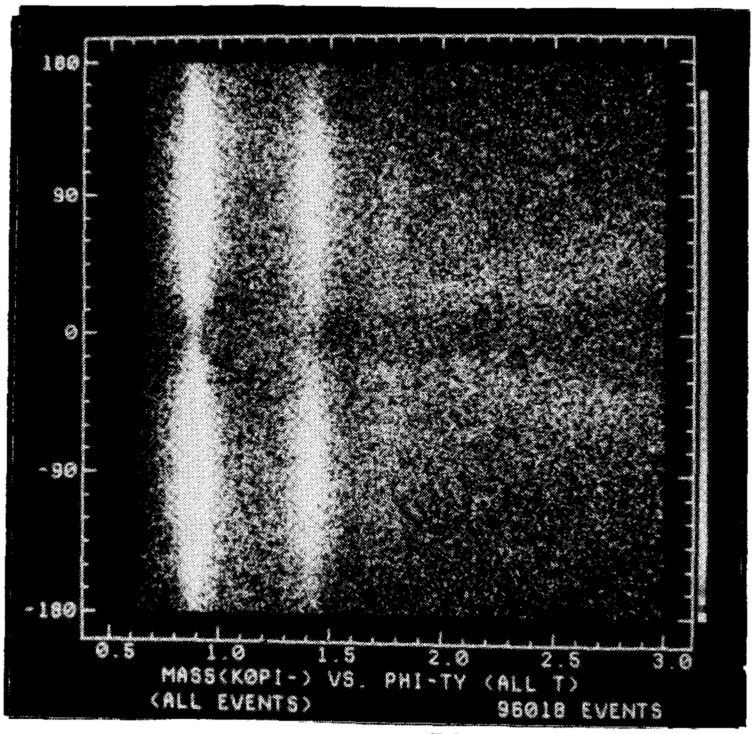

Figure 7. The decay distribution of $K^{*-} \to \bar{K}^0\pi^-$ is shown in a scatterplot of the azimuthal (Treiman–Yang) angle as a function of $K\pi$ mass.

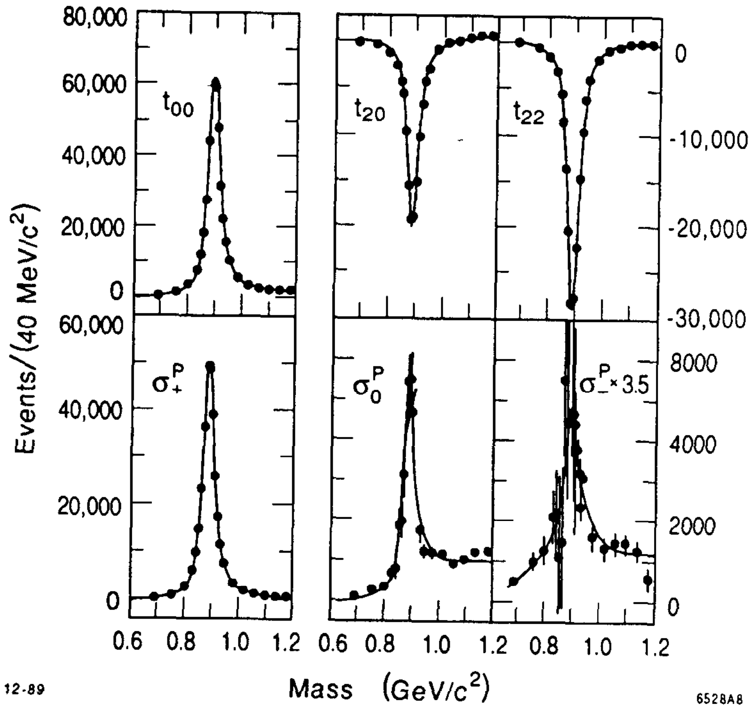

Figure 8. The moments for the process $K^-p \to K^{*-}p$; $K^{*-} \to \bar{K}^0\pi^-$ in the region around $K\pi$ mass of 1 GeV/c^2. For details see Ref. 6.

function of $K\pi$ mass; the cosine of the Jackson angle in the $K\pi$ center-of-mass is shown in Fig. 6, while the azimuthal Treiman–Yang angle is shown in Fig. 7. Clear indications of the spin 1, natural parity exchange are seen, as are the $J^P = 1^- \; 2^+$, 3^- of the three leading K^* states at 890, 1420, and 1780 MeV/c^2.

Table 1: Breit–Wigner parameters for the $K^*(892)$ region. The first error is statistical, the second systematic.

Fit	Mass (MeV/c^2)	Width (MeV/c^2)	Radius (GeV/c^{-1})
t_{00}	$890.9 \pm 0.2 \pm 0.5$	$46.2 \pm 0.5 \pm 0.5$	$5.6 \pm 0.5 \pm 1.0$
t_{20}	$889.6 \pm 0.5 \pm 0.5$	$50.7 \pm 1.4 \pm 0.5$	$100. \pm 50. \pm 5.0$
t_{22}	$890.5 \pm 0.3 \pm 0.5$	$46.0 \pm 0.7 \pm 0.5$	$11.4 \pm 2.5 \pm 1.0$
σ_0^P	$890.3 \pm 0.2 \pm 0.5$	$50.4 \pm 1.7 \pm 0.5$	$0.0 \pm 10. \pm 1.0$
σ_+^P	$890.7 \pm 0.2 \pm 0.5$	$46.4 \pm 0.4 \pm 0.5$	$15.4 \pm 5. \pm 1.0$
σ_-^P	$898.8 \pm 7.7 \pm 0.5$	$87.9 \pm 30. \pm 3.0$	$100. \pm 50. \pm 5.0$

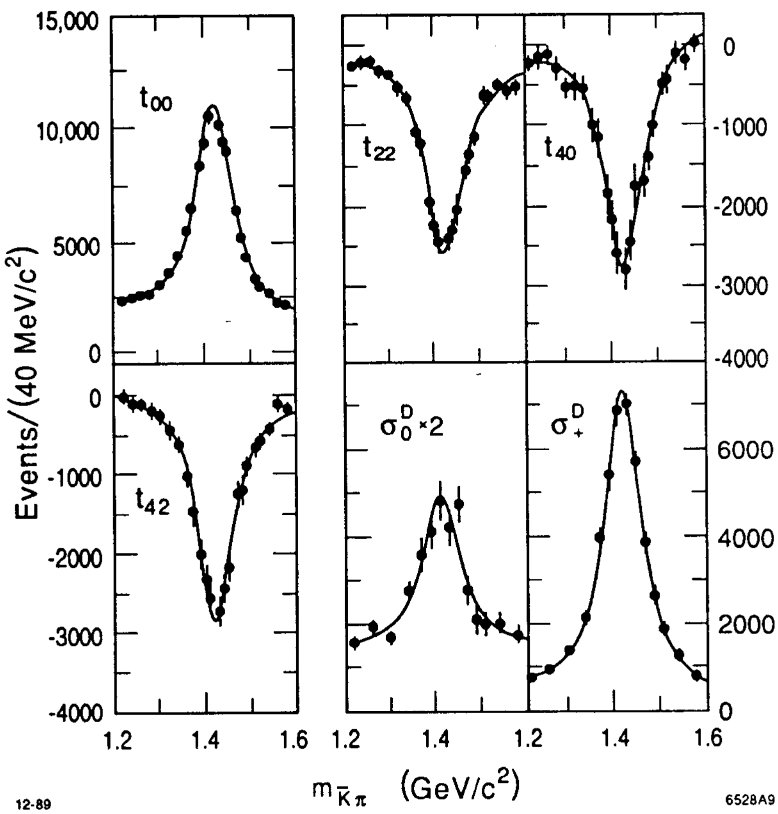

Figure 9. The moments for the reaction $K^-p \to K^{*-}p$; $K^{*-} \to \bar{K}^0\pi^-$ in the region around $K\pi$ mass of 1400 MeV/c^2.

A more quantitative analysis yields the moments of the $K\pi$ decay distribution in the three mass regions of interest. Figure 8 gives the moments in the region around 1 GeV/c^2 —the region dominated by the production and decay of the $K^*(892)$. The parameters of the $K^*(892)$ Breit–Wigner line shape, as obtained from fits to the different moments, are summarized in Table 1, and described in detail in Ref. 6. Figure 9 shows the behavior of the moments in the 1400 MeV/c^2 region, and Fig. 10 shows the moments in the 1800 MeV/c^2 region. Tables 2 and 3 give the resonance parameters from fits to

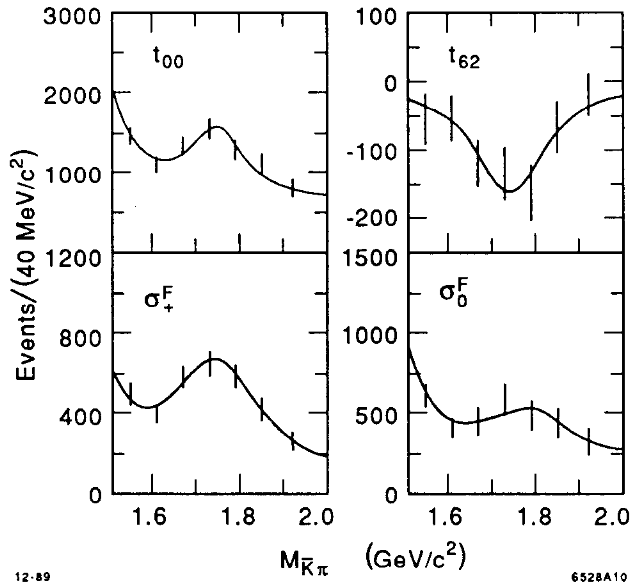

Figure 10. The moments for the process $K^-p \to K^{*-}p$, $K^{*-} \to \bar{K}^0\pi^-$ in the region around $K\pi$ mass of 1750 MeV/c^2.

Table 2: Breit–Wigner parameters for the $K_2^*(1430)$ region. The first error is statistical, the second systematic.

Fit	Mass (MeV/c²)	Width (MeV/c²)	Radius (GeV/c⁻¹)
t_{00}	$1419 \pm 0.8 \pm 1$	$99.3 \pm 3.0 \pm 2$	$100 \pm 78 \pm 10$
t_{22}	$1424 \pm 2.6 \pm 1$	$100.7 \pm 10.1 \pm 3$	$0 \pm 53 \pm 5$
t_{40}	$1424 \pm 3.5 \pm 1$	$101 \pm 11.3 \pm 3$	$5 \pm 5 \pm 3$
t_{42}	$1420 \pm 2 \pm 1$	$89.8 \pm 5 \pm 1$	$3.1 \pm 1.2 \pm 1$
σ_0^D	$1412 \pm 4.8 \pm 1$	$100.7 \pm 14.7 \pm 3$	$100 \pm 59 \pm 15$
σ_+^D	$1420.5 \pm 1.1 \pm 1$	$98.8 \pm 4.4 \pm 3$	$12.5 \pm 54 \pm 10$

Table 3: Breit–Wigner parameters for the $K_3^*(1780)$ region. The first error is statistical, the second systematic.

Fit	Mass (MeV/c²)	Width (MeV/c²)	Radius (GeV/c⁻¹)
t_{00}	$1747 \pm 12 \pm 4$	$145 \pm 59 \pm 10$	100
t_{62}	$1738 \pm 21 \pm 5$	$195 \pm 36 \pm 15$	100
σ_0^F	$1784 \pm 43 \pm 10$	$233 \pm 360 \pm 50$	100
σ_+^F	$1741 \pm 9.8 \pm 5$	$243 \pm 60 \pm 10$	100

these moments, as described in Ref. 6. Figure 11 shows the leading natural spin-parity amplitudes and Table 4 gives the best estimates for the parameters of the three leading K^* resonances.

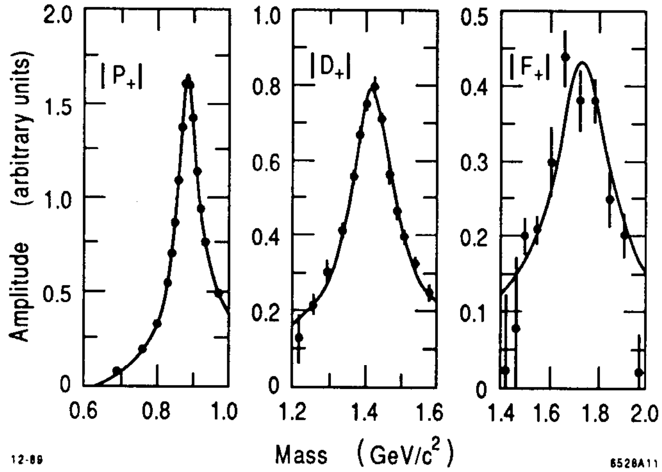

Figure 11. The leading natural J^P exchange amplitudes. The scale is arbitrary (see text), but the errors indicate the relative statistical precision of each measurement.

Table 4: The leading natural spin-parity amplitudes. A single Breit–Wigner resonance is assumed for each wave.

Resonance	Mass (GeV/c^2)	Width (GeV/c^2)	Radius (GeV/c^{-1})
$K^*(892)$	$0.8904 \pm 0.0002 \pm 0.0005$	$0.0452 \pm 0.001 \pm 0.002$	$12.1 \pm 3.2 \pm 3$
$K_2^*(1430)$	$1.4234 \pm 0.002 \pm 0.003$	$0.098 \pm 0.004 \pm 0.004$	$4.8 \pm 2.3 \pm 3$
$K_3^*(1780)$	$1.720 \pm 0.010 \pm 0.015$	$0.187 \pm 0.031 \pm 0.020$	$8.5 \pm 3 \pm 10$

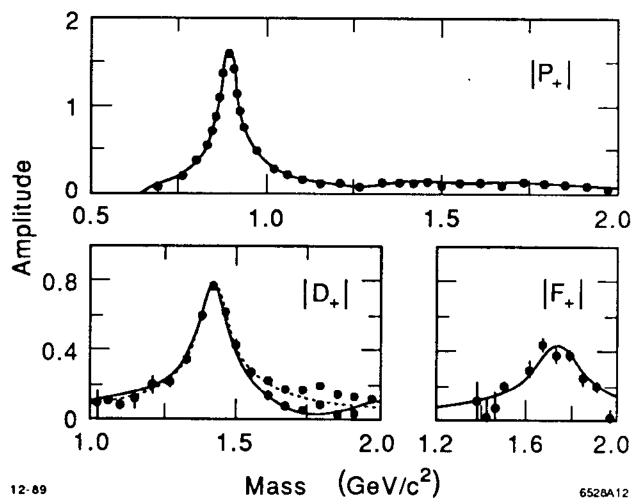

Figure 12. The mass dependence of the P, D and F-waves from threshold up to 2 GeV/c^2.

Having examined the leading amplitudes, we can now explore the structure in the underlying waves. The mass dependence of the natural parity exchange amplitudes from threshold to 2 GeV/c^2 is shown in Fig. 12. The relative phase between the P- and D-waves and between the D and F-waves is shown in Fig. 13, and indicates the presence of resonant waves in addition to the leading K^*'s. This data has been fit using the superposition of

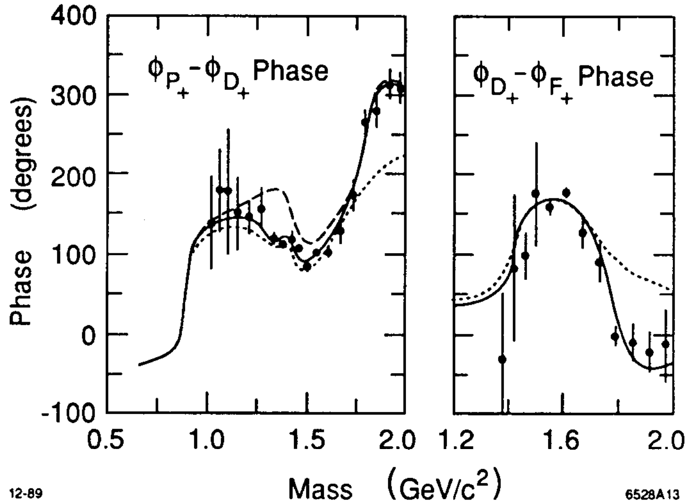

Figure 13. The energy dependence of the phase difference between the P, D and the D, F-waves in the process $K^-p \to K^{*-}p$.

Table 5: The P and D-wave resonance parameters.

Wave	Mass (GeV/c²)	Width (GeV/c²)	Phase (deg.)
1^-	0.8905 (fixed)	0.045 (fixed)	0 (fixed)
	1.367 ± 0.054	0.114 ± 0.101	69 ± 7
	1.678 ± 0.064	0.454 ± 0.270	-92 ± 17
2^+	1.425 (fixed)	0.1 (fixed)	40 ± 4
	1.978 ± 0.040	0.398 ± 0.047	2 ± 5

interfering resonant amplitudes with arbitrary relative production phases; the result is shown as the solid curve in Figs. 12 and 13.

The dashed curve in Fig. 13 shows the behavior of the P–D phase, if the 1700 MeV/c² P-wave state is excluded. Similarly, the dotted curve shows the expected phase behavior if the D-wave state at 1980 MeV/c² is excluded. The parameters of the underlying resonances from this analysis are given in Table 5. The parameters for the two underlying P-wave states, and the D-wave state, are in good agreement with those obtained in our previous analysis of reactions (1) and (2).[2,3,5] This is independent confirmation of the radial excitation of the $K_2^*(1420)$ at 1980 MeV/c², and of the P-wave states—the radial excitation of the $K^*(892)$ at $\sim$ 1400 MeV/c² and the $^3D_1$ member of the $L = 2$ triplet associated with the $K_3^*(1780)$.

CONCLUSION

The LASS group is continuing its systematic study of K^* spectroscopy, using the high-statistics data on 11 GeV/c² / c K^-p interactions obtained at SLAC. The most recent study of the reaction $K^- p \rightarrow \bar{K}^0 \pi^- p$ has resulted in confirmation of two new P-wave states, and the probable radial excitation of the $K_2^*(1420)$ at a mass of $\sim$ 1950 MeV/c^2. Currently, work is in progress on the analysis of $K\phi$ and $K\omega$ final states.

REFERENCES

1. B. Ratcliff, Invited talk at HADRON89, Ajaccio, France, Sept. 23–27, 1989; SLAC–PUB–5150.
2. $K^- \pi^+$: Aston et al, Nucl. Phys. **B296** (1988) 493; *ibid* **B180** (1986) 308.
3. $K^* \pi$, $K\rho$: Aston et al, Nucl. Phys. **B292** (1987) 693.
4. $K^- \eta$: Aston et al, Phys. Lett. **B201** (1988) 169.
5. Aston et al, SLAC–PUB–4652 (1988); SLAC–PUB–4202 (1987).
6. F. Bird, SLAC–Report–332, Stanford University Ph.D. thesis.